



Contents lists available at ScienceDirect

Environmental Pollution

journal homepage: www.elsevier.com/locate/envpol

Internal dynamics of inorganic and methylmercury in a marine fish: Insights from mercury stable isotopes



Bong Joo Lee ^a, Sae Yun Kwon ^{b, c, *}, Runsheng Yin ^d, Miling Li ^e, Saebom Jung ^b,
Seung Hyeon Lim ^f, Ju Hyeon Lee ^b, Kang Woong Kim ^g, Kyoung Duck Kim ^g, Ji Won Jang ^a

^a Aquafeed Research Center, National Institute of Fisheries Science, 2600 Haean-Ro, Nam Gu, Pohang, 37517, South Korea

^b Division of Environmental Science and Engineering, Pohang University of Science and Technology, 77 Cheongam-Ro, Nam Gu, Pohang, 37673, South Korea

^c Institute for Convergence Research and Education in Advanced Technology, Yonsei University, 85 Songdogwahak-Ro, Yeonsu-Gu, Incheon, 21983, South Korea

^d State Key Laboratory of Ore Deposit Geochemistry, Institute of Geochemistry, Chinese Academy of Sciences, Guiyang, 550081, China

^e School of Marine Science and Policy, University of Delaware, 261 S. College Avenue, Newark, DE, 19716, USA

^f Department of Chemical Engineering, Pohang University of Science and Technology, 77 Cheongam-Ro, Nam Gu, Pohang, 37673, South Korea

^g Aquaculture Management Division, National Institute of Fisheries Science, 216 Gijanghaean-Ro, Gijang-Gun, Busan, 4608, South Korea

ARTICLE INFO

Article history:

Received 1 March 2020

Received in revised form

25 August 2020

Accepted 31 August 2020

Available online 11 September 2020

Keywords:

Mercury

Stable isotope

Fish

Monitoring

Internal distribution

ABSTRACT

Mercury isotope ratios in fish tissues have been used to infer sources and biogeochemical processes of mercury in aquatic ecosystems. More experimental studies are however needed to understand the internal dynamics of mercury isotopes and to further assess the feasibility of using fish mercury isotope ratios as a monitoring tool. We exposed Olive flounder (*Paralichthys olivaceus*) to food pellets spiked with varying concentrations (400, 1600 ng/g) of methylmercury (MeHg) and inorganic mercury (IHg) for 10 weeks. Total mercury (THg), MeHg concentrations, and mercury isotope ratios ($\delta^{202}\text{Hg}$, $\Delta^{199}\text{Hg}$, $\Delta^{200}\text{Hg}$) were measured in the muscle, liver, kidney, and intestine of fish. Fish fed mercury unamended food pellets and MeHg amended food pellets showed absence of internal $\delta^{202}\text{Hg}$ and $\Delta^{199}\text{Hg}$ fractionation in all tissue type. For fish fed IHg food pellets, the $\delta^{202}\text{Hg}$ and $\Delta^{199}\text{Hg}$ values of intestine equilibrated to those of the IHg food pellets. Kidney, muscle, and liver exhibited varying degrees of isotopic mixing toward the IHg food pellets, consistent with the degree of IHg bioaccumulation. Liver showed additional positive $\delta^{202}\text{Hg}$ shifts ($\sim 0.63\%$) from the binary mixing line between the unamended food pellets and IHg food pellets, which we attribute to redistribution or biliary excretion of liver IHg with a lower $\delta^{202}\text{Hg}$ to other tissues. Significant $\delta^{202}\text{Hg}$ fractionation in the liver and incomplete isotopic equilibration in the muscle indicate that these tissues may not be suitable for source monitoring at sites heavily polluted by IHg. Instead, fish intestine appears to be a more suitable proxy for identifying IHg sources. The results from our study are essential for determining the appropriate fish tissues for monitoring environmental sources of IHg and MeHg.

© 2020 Elsevier Ltd. All rights reserved.

1. Introduction

Speciation and concentration analyses of mercury in fish tissues have been used to monitor the extent of pollution and ecosystem fate of mercury in aquatic environments (e.g., Eagle-Smith et al., 2015). Anthropogenic activities release mercury dominantly in

the form of inorganic mercury (IHg; Streets et al., 2019). Microbial methylation of IHg in the water column and surface sediments can lead to the production of a toxic form of mercury known as methylmercury (MeHg; Blum et al., 2013; Eckley et al., 2006; Gilmour et al., 1992). MeHg, upon uptake by fish, is rapidly assimilated and distributed to various tissues by crossing cellular membranes (Leaner and Mason, 2004; Rabenstein and Evans, 1978). MeHg has a long internal half-life (~ 2 yrs) in the muscle owing to the strong binding affinity with sulfur-containing ligands (McCloskey et al., 1998; Oliveira Ribeiro et al., 1999). IHg, by contrast, is excreted rapidly from biological tissues and elevated IHg levels in fish have been reported primarily at mercury

* Corresponding author. Division of Environmental Science and Engineering, Pohang University of Science and Technology, 77 Cheongam-Ro, Nam Gu, Pohang, 37673, South Korea.

E-mail address: saeyunk@postech.ac.kr (S.Y. Kwon).

contaminated sites (Cizdziel et al., 2003; Donovan et al., 2016). Elevated liver to muscle total mercury (THg) ratios (>1) have been observed at sites contaminated by metallic mercury given the rapid response of liver to environmental IHg exposure (Evans et al., 1993; Rua-Ibarz et al., 2019).

Previous studies have also used fish mercury concentration and speciation to investigate the internal processes of mercury and have shown conflicting conclusions. For instance, Wang et al. (2017) exposed marine fish to dietary MeHg and observed a 2-fold increase in the whole-body IHg concentration. The authors attributed this to the demethylation of dietary MeHg in the intestine of fish. In contrast, Wang et al. (2013) observed simultaneous reductions in fish liver MeHg and THg concentrations and increases in muscle MeHg and THg concentrations and suggested that this reflects mercury redistribution from liver to muscle rather than internal demethylation. The evidence of IHg methylation, based on the measurable conversion of IHg labeled stable isotopes (^{198}IHg) into $^{198}\text{MeHg}$, has also been reported in the intestines of fish (Rudd et al., 1980; Wang et al., 2013).

The measurement of natural abundances of mercury isotopes has been used to assess sources and processes governing the environmental and biological fate of mercury (e.g., Blum et al., 2014; Kwon et al., 2020). While many environmentally relevant processes including methylation, demethylation (Kritee et al., 2009; Rodríguez-González et al., 2009), and thiol-ligand exchange (Wiederhold et al., 2010) result in mass-dependent fractionation (MDF; reported as $\delta^{202}\text{Hg}$), significant mass-independent fractionation of odd-mass number isotopes (MIF_{odd} ; reported as $\Delta^{199}\text{Hg}$) have been observed primarily during photochemical reduction and degradation of IHg and MeHg, respectively (Bergquist and Blum, 2007; Zheng and Hintelmann, 2009). Significant MIF of even-mass number isotopes (MIF_{even} ; reported as $\Delta^{200}\text{Hg}$) is thought to occur via photochemical oxidation of Hg^0 in the atmosphere (Chen et al., 2012; G. Sun et al., 2016) and few environmental samples of precipitation, seawater, plankton, and fish have reported significantly positive $\Delta^{200}\text{Hg}$ values (e.g., Blum and Johnson, 2017).

Thus far, fish mercury isotope ratios have been used extensively to identify environmental sources and biogeochemical processes of mercury in diverse aquatic ecosystems (e.g., Blum et al., 2013; Cransveld et al., 2017; Lepak et al., 2018; Kwon et al., 2014; Sherman and Blum, 2013). Recent studies have also illustrated the potential of using mercury isotope ratios in fish and mammalian tissues to investigate the internal processes governing the body burden and the distribution of speciated mercury (Bolea-Fernandez et al., 2019; Feng et al., 2015; Kwon et al., 2012, 2013, 2016; Li et al., 2020; Masbou et al., 2018; Perrot et al., 2016, 2019; Rua-Ibarz et al., 2019; Xu and Wang, 2015). In the case of fish, Kwon et al. (2012) first conducted feeding experiments and showed absence of MDF and MIF_{odd} during MeHg trophic transfer to the muscle tissues of fish. The following experimental studies measured mercury isotope ratios in multiple fish tissues and observed significant internal MDF in some fish, which was attributed to either internal demethylation in the intestine or redistribution of mercury from the liver (Feng et al., 2015; Kwon et al., 2013). Recent field observations reported higher $\delta^{202}\text{Hg}$ values in the muscle compared to liver, which were explained by internal demethylation in the liver followed by the distribution MeHg with a higher $\delta^{202}\text{Hg}$ to the muscle (Perrot et al., 2019; Rua-Ibarz et al., 2019). More controlled experimental studies are needed to understand precisely the internal processes leading to mercury isotope distribution and fractionation in and across fish tissues and to better use fish mercury isotope ratios as a monitoring tool.

We conducted controlled feeding experiments by exposing

Paralichthys olivaceus (Olive flounder) to food pellets spiked with either IHg or MeHg to understand tissue-specific variation in mercury isotope ratios at different exposure scenarios. Olive flounder is a highly abundant and commercially valuable species in many East Asian countries including South Korea, China, and Japan (Choi et al., 2011). They are found at a wide range of depths (10–200 m) and environments spanning from coastal to open ocean. Olive flounder is characterized as an opportunistic bottom feeder by feeding on various prey items including small fish, crustaceans, mollusks, and fish eggs (Choi et al., 2011). The results from our study are essential for determining the appropriate tissues of Olive flounder and other species of marine fish for monitoring environmental sources of IHg and MeHg.

2. Materials & methods

2.1. Fish feeding experiment

Olive flounder weighing approximately 10 g were obtained from a commercial fish farm located at Taean province, South Korea in the spring of 2016. The fish were transported and acclimatized at the Aquafeed Research Center, National Institute of Fisheries Science, South Korea for one month. During the period of acclimatization, the fish were fed food pellets composed mainly of anchovy and pompano (70% dry weight), which were caught at the west coast of Chile and Peru. Anchovy and pompano were freeze-dried, homogenized, pelleted with the addition of a cellulose-based premix and distilled water (30% v/v), and evaporated to dryness in an oven (60 °C) for 2 h. All fish were raised in indoor PVC tanks (300 L capacity) with no natural sunlight. The PVC tanks were maintained by a flow-through system to continuously circulate new water and to remove suspended residues (i.e., feces and unconsumed food pellets). All tanks were maintained at a constant temperature of 24.5 ± 2.7 °C and salinity of $33 \pm 1\%$.

Prior to the experiment, Olive flounder weighing approximately 21.1 ± 0.4 g were randomly distributed into five different treatments with 3 replicate tanks for each treatment. The treatment in which the fish were continued to be fed with mercury unamended food pellets are referred to as control. Fish fed with food pellets that were manipulated to two different MeHg and IHg concentrations are referred to as MeHg_high (1600 ng/g), MeHg_low (400 ng/g), IHg_high (1600 ng/g), and IHg_low (400 ng/g). The mercury amended food pellets were prepared by soaking them in either synthetic MeHg (CH_3ClHg , Sigma-Aldrich) or synthetic IHg (HgCl_2 , Sigma-Aldrich) solution for 2 d followed by evaporation in an oven for 2 h. All food pellets were kept at -20 °C prior to use.

Fish were fed twice a day with their respective food pellets for 10 weeks. After the feeding experiment, all fish achieved similar body weight (124 ± 7 g) regardless of the treatment. We did not observe any fish mortality during or after the experiment. Three individuals were randomly selected per treatment and from different tanks and euthanized by tricaine methanesulphonate (MS-222, 200 $\mu\text{g/g}$). Fish were dissected for muscle, liver, kidney, and intestine at the Environmental Health Assessment Laboratory, Division of Environmental Science and Engineering, Pohang University of Science and Technology (POSTECH), South Korea. The liver and kidney tissues of an individual fish had small sample mass and did not contain enough mercury for the analyses, so samples were pooled from the tissues of three individuals from each treatment. Among those dissected for liver and kidney, we chose one to three individual fish and dissected them for muscle and intestine tissues. The muscle and intestine tissues were kept as individual fish. The dissection was performed using stainless steel scalpels and scissors, which were cleaned with distilled water and alcohol between samples to avoid contamination. The intestine

samples were washed thoroughly with distilled water to remove undigested food pellets. Either pooled or individual fish tissue as well as food pellets were placed in an acid-washed glass vial and frozen at -20°C . The fish tissues and food pellets were freeze-dried and homogenized with mortar and pestle.

2.2. Mercury concentration analyses

The complete sample size and the results of the individual or replicate analyses of THg and MeHg concentration and mercury isotope ratios are shown in Table S1. Each individual muscle and intestine samples was subsampled appropriately for THg and MeHg concentration and mercury isotope ratios. Both THg and MeHg concentrations were measured at the Environmental Health Assessment Laboratory, POSTECH. The THg concentrations were determined by atomic absorption spectroscopy (AAS) using a Nippon Instruments MA-3000 Hg analyzer. The THg of some individual muscle and intestine samples and all pooled kidney, liver, and food pellet samples were measured twice and their relative standard deviation was within 12% (Table S1). Standard reference material ERM CE 464 (tuna fish) was measured between samples for quality control and quality assurance. The recoveries of THg in ERM CE 464 were between 91 and 102% ($n = 7$).

For MeHg, the homogenized samples were digested in a 5 mL potassium hydroxide and methanol mixture (1:4, v/v) for 6 h at 70°C . The digested samples were measured using a cold vapor atomic fluorescent spectrometry (CV-AFS; Brooks Rand Model III Hg detector) coupled with a gas column (GC). The method used to measure MeHg concentration is described in Hammerschmidt and Fitzgerald (2006). Standard reference material ERM CE 464 ($n = 8$) and TORT-3 (lobster; $n = 1$) were measured between samples and the recoveries of MeHg were between 82 and 98% and 92%, respectively. The proportion of MeHg is reported as % MeHg (MeHg concentration/THg concentration $\times 100\%$).

2.3. Mercury isotope analyses

Mercury isotope ratios were measured at the State Key Laboratory of Ore Deposit Geochemistry, Institute of Geochemistry, Chinese Academy of Sciences, China. Approximately 0.2–0.4 g of freeze-dried samples were digested in a 5 mL aqua regia followed by the addition of 0.2 mL bromine chloride for 12 h at 95°C . After digestion, 0.5 mL of hydroxylamine hydrochloride solution was added to degrade the residual bromine chloride. The samples were then diluted to THg concentration of 0.5 ng/mL and acidity of 20% and were measured using a Neptune Plus multi-collector inductively coupled plasma mass spectrometer (MC-ICP-MS) following a previous method (Yin et al., 2016). Sample mercury was introduced to the instrument by continuously reducing Hg^{2+} with 3% SnCl_2 and separating Hg^0 using a glass-liquid phase separator. Instrumental mass bias was corrected using the NIST SRM 997 Tl standard

(diluted to 50 ng/mL Tl in 3% HNO_3 solution). The samples were bracketed with NIST SRM 3133 and by matching the THg concentration and the acid matrix. MDF is reported as $\delta^{202}\text{Hg}$ (in units of ‰) referenced to NIST SRM 3133 (Blum and Bergquist, 2007):

$$\delta^{202}\text{Hg} = \left\{ \left[\left(\frac{{}^{202}\text{Hg}/{}^{198}\text{Hg}}{\text{sample}} \right) / \left(\frac{{}^{202}\text{Hg}/{}^{198}\text{Hg}}{\text{NIST3133}} \right) - 1 \right] \times 1000 \right\} \quad (1)$$

MIF represents the difference between the measured $\delta^{\text{xxx}}\text{Hg}$ value and the value predicted based on MDF and the $\delta^{202}\text{Hg}$ value. MIF is reported as $\Delta^{199}\text{Hg}$, $\Delta^{200}\text{Hg}$, and $\Delta^{201}\text{Hg}$ (in units of ‰) and calculated using the following equations (Blum and Bergquist, 2007):

$$\Delta^{199}\text{Hg} = \delta^{199}\text{Hg} - \left(\delta^{202}\text{Hg} \times 0.2520 \right) \quad (2)$$

$$\Delta^{200}\text{Hg} = \delta^{200}\text{Hg} - \left(\delta^{202}\text{Hg} \times 0.5024 \right) \quad (3)$$

$$\Delta^{201}\text{Hg} = \delta^{201}\text{Hg} - \left(\delta^{202}\text{Hg} \times 0.7520 \right) \quad (4)$$

Analytical uncertainty at 2SD is estimated based on either replicate analyses of the standard solution NIST SRM 3177 (also known as the commercial version of UM-Almadén secondary standard solution; $n = 16$) or replicate analyses of standard reference material ERM CE 464 ($n = 10$). We used ERM CE 464 to report the analytical uncertainty since it had the larger uncertainty. ERM CE 464 had mean values ($\pm 2\text{SD}$) of $\delta^{202}\text{Hg} = 0.70 \pm 0.14\text{‰}$, $\Delta^{201}\text{Hg} = 1.96 \pm 0.10\text{‰}$, $\Delta^{200}\text{Hg} = 0.08 \pm 0.08\text{‰}$, and $\Delta^{199}\text{Hg} = 2.37 \pm 0.14\text{‰}$, which are similar to those reported in previous studies (Blum et al., 2013; Gehrke et al., 2011; Kwon et al., 2012, 2013; 2014, 2015; Li et al., 2014; Sherman and Blum, 2013). NIST SRM 3177 had mean values ($\pm 2\text{SD}$) of $\delta^{202}\text{Hg} = -0.53 \pm 0.12\text{‰}$, $\Delta^{201}\text{Hg} = -0.05 \pm 0.08\text{‰}$, $\Delta^{200}\text{Hg} = -0.01 \pm 0.10\text{‰}$, and $\Delta^{199}\text{Hg} = -0.02 \pm 0.10\text{‰}$. We compiled mercury isotope ratios of NIST SRM 3177 from prior studies (Chen et al., 2012; Cransveld et al., 2017; Kwon et al., 2015; Laffont et al., 2011; Lepak et al., 2018; Li et al., 2014; Masbou et al., 2018; Yin et al., 2016) and observed consistent average values ($\delta^{202}\text{Hg} = -0.54 \pm 0.11\text{‰}$, $\Delta^{201}\text{Hg} = -0.06 \pm 0.07\text{‰}$, $\Delta^{200}\text{Hg} = 0.01 \pm 0.06\text{‰}$, and $\Delta^{199}\text{Hg} = -0.02 \pm 0.07\text{‰}$, $n = 280$).

3. Results & discussion

3.1. Mercury concentrations in fish and food pellets

The average THg concentration of the food pellets unamended with mercury (control) and those spiked with varying concentrations of IHg (IHg_low, IHg_high) and MeHg (MeHg_low,

Table 1

Average THg concentrations (ng/g) and average % MeHg values of the food pellets and the tissues of Olive flounder from different treatments. The average THg concentrations of liver and kidney tissues are from pooled samples (3 individuals). The average THg concentrations of intestine and muscle tissues are from individual samples.

	Control		MeHg_low		MeHg_high		IHg_low		IHg_high	
	THg	% MeHg	THg	% MeHg	THg	% MeHg	THg	% MeHg	THg	% MeHg
Food pellet	49	85	404	60	1555	95	435	20	1471	6
Liver	35	106	503	85	2675	89	153	41	247	41
Intestine	88	75	915	83	3612 ^b	82	740 ^d	19	5152 ^e	7
Kidney	70	97	975	78	3261	95	98	70	266	63
Muscle	106	75 ^a	1257	100	4431 ^c	99	93	59	145	38

^{a,b,c,d,e} The average % MeHg values are based on two separate THg and MeHg measurements. The average % MeHg values of the remaining samples are based on one or two THg measurements and one MeHg measurement from the same sample. Refer to Table S1 for more detail.

MeHg_high) are summarized in Table 1. The mercury unamended food pellets showed low THg concentrations, similar to the natural diets of Olive flounder and those reported in commercial food pellets composed of marine fish by-product (Feng et al., 2015; Kwon et al., 2012). The food pellets spiked with IHg and MeHg confirmed that all treatments were prepared in the expected concentrations. The % MeHg (THg present as MeHg) of the MeHg_low food pellets (~60%) suggests that they have failed to equilibrate properly to synthetic MeHg and/or has undergone MeHg degradation, which we discuss further in the sections below.

The tissues of fish from the control treatment fed food pellets unamended with mercury showed relatively low THg concentrations (range; 34–132 ng/g) and % MeHg values, similar to the control food pellets (range; 72–106%; Table 1). After 10 weeks of dietary exposure, the fish from the MeHg_low and MeHg_high treatments showed 10- to 14-fold and 41- to 76-fold higher THg concentrations, respectively, and small changes in % MeHg compared to control (Table 1). In contrast, the tissues of fish from the IHg_low and IHg_high treatments (except for intestine) showed relatively small increases in THg concentrations—1- to 4-fold and 2- to 7-fold higher THg concentrations compared to control, respectively—and reductions in % MeHg (Table 1). Particularly large increases in THg concentrations (8- to 59-fold higher) and large reductions in % MeHg were observed in the intestine. This suggests that, while dietary MeHg is efficiently assimilated and bioaccumulated into fish, a large proportion of dietary IHg accumulated in the intestine is excreted rather than being bioaccumulated into fish tissues.

The liver to muscle THg ratio of fish (liver THg concentration/muscle THg concentration) has been used to quantify the degree of IHg exposure and previous studies documented a ratio >1 at sites impacted by anthropogenic activities (Cizdziel et al., 2003; Rua-Ibarz et al., 2019). The average liver to muscle THg ratios of the control and MeHg treatments were 0.4 (control), 0.4 (MeHg_low), and 0.6 (MeHg_high). The average liver to muscle THg ratios in the IHg treatments were 1.6 (IHg_low) and 1.7 (IHg_high). Our results are consistent with previous studies, which suggested that fish liver responds rapidly to IHg exposure and it can serve as a bioindicator for IHg pollution (Evans et al., 1993).

3.2. Isotopic compositions of the control treatment

The mercury unamended food pellets and fish from the control treatment showed highly positive mercury isotope ratios ($\delta^{202}\text{Hg}$, $\Delta^{199}\text{Hg}$, $\Delta^{200}\text{Hg}$) relative to the MeHg and IHg treatments (Fig. 1A). We also observed significant variations in $\delta^{202}\text{Hg}$ and $\Delta^{199}\text{Hg}$ among the tissues, in which the kidney and liver composed of higher % MeHg (97–106%) displayed higher $\delta^{202}\text{Hg}$ and $\Delta^{199}\text{Hg}$ compared to the food pellets, muscle, and intestine with lower % MeHg (72–85%). Natural environmental samples of sediment and fish have shown higher $\delta^{202}\text{Hg}$ and $\Delta^{199}\text{Hg}$ in MeHg compared to IHg (Entwisle et al., 2018; Epov et al., 2008; Janssen et al., 2015). By plotting % MeHg against $\delta^{202}\text{Hg}$ and $\Delta^{199}\text{Hg}$ of the fish tissues, we estimate that the MeHg fractions in the fish tissues explain 76% and 87% of the $\delta^{202}\text{Hg}$ and $\Delta^{199}\text{Hg}$ variation, respectively (all $p < 0.05$; Figure S1). While our result relies on a small sample size, our observation is consistent with previous studies that have attributed the variation in mercury isotope ratios to the differences in MeHg fractions across fish tissues (Kwon et al., 2012, 2013).

While many experimental and field studies have confirmed the absence of MIF_{odd} during internal processes (Feng et al., 2015; Kwon et al., 2012, 2013; Li et al., 2020; Masbou et al., 2018; Perrot et al., 2016, 2019; Rua-Ibarz et al., 2019), the potential MDF in fish still remains a question. Feng et al. (2015) fed fish with food pellets unamended with mercury (~80% MeHg, 60 ng THg/g) and observed a consistent $\Delta^{199}\text{Hg}$ and a much lower $\delta^{202}\text{Hg}$ in the feces (mostly IHg) compared to the estimated $\delta^{202}\text{Hg}$ of IHg in the food pellets. The authors attributed this to MDF possibly via internal demethylation, which produces a lower $\delta^{202}\text{Hg}$ in the excreted IHg. While the bioaccumulation of the residual MeHg with a higher $\delta^{202}\text{Hg}$ would expect to increase $\delta^{202}\text{Hg}$ in the fish tissues, the authors observed similar $\delta^{202}\text{Hg}$ between the fish and the food pellets (Feng et al., 2015). This suggests that the potential MDF caused by internal processes including demethylation may be diluted by the isotopic composition of dietary MeHg given that MeHg is efficiently assimilated and distributed to various tissues of fish. Furthermore, the tissue-specific variation in mercury isotope ratios resulted primarily by the varying MeHg fraction and upon exposure to low THg concentration (~49 ng/g) and elevated % MeHg diet (~85%; similar to natural diet) in our control fish suggest that the isotopic composition of dietary MeHg source is well retained in the fish

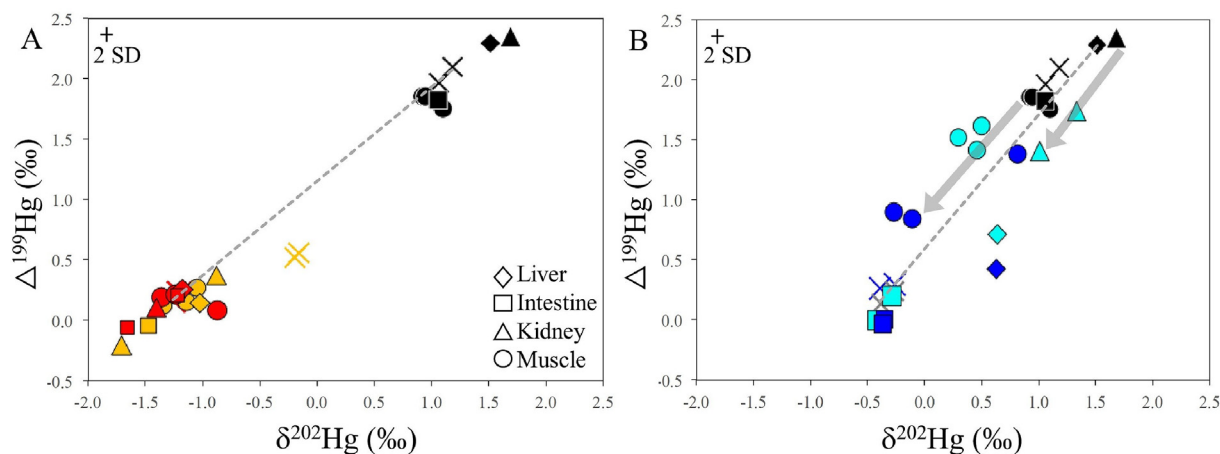


Fig. 1. $\delta^{202}\text{Hg}$ and $\Delta^{199}\text{Hg}$ of the fish tissues from A) the control (black), MeHg_low (yellow), and MeHg_high treatments (red), and B) the control (black), IHg_low (bright blue), and IHg_high treatments (dark blue). Individual data point of liver and kidney represents a sample pooled from three individual fish. Individual data point of muscle and intestine represents a sample from one individual fish. The food pellets are shown in cross symbols. Grey dashed line in panel A represents a binary mixing between the control and MeHg_high food pellets. Grey arrows in panel B represent the isotopic shifts of the muscle and kidney from the control toward the IHg food pellets. Analytical uncertainty is shown as 2SD.

tissues.

The highly positive $\delta^{202}\text{Hg}$ and $\Delta^{199}\text{Hg}$ observed in the control food pellets composed mainly of natural anchovy and pompano (see *Methods and materials* section) and the tissues of control fish are within the ranges of natural marine fish ($\delta^{202}\text{Hg} = -2.09$ to 1.84‰ , $\Delta^{199}\text{Hg} = 0.03$ to -5.50‰ ; reviewed in Kwon et al., 2020). Previous studies have collectively suggested that the positive $\delta^{202}\text{Hg}$ and particularly the positive $\Delta^{199}\text{Hg}$ in marine fish reflect MeHg that has undergone photochemical degradation prior to bioaccumulation into fish (e.g., Blum et al., 2013; Kwon et al., 2014). The fact that the elevated $\delta^{202}\text{Hg}$ and $\Delta^{199}\text{Hg}$ are shown in both the food pellets and the control fish suggests that the mercury isotope ratios of the control food pellets, reflecting MeHg that has undergone photochemical degradation and bioaccumulation into anchovy and pompano from their natural habitat, are transferred to the tissues of the control fish via trophic transfer during the feeding experiment.

In regards to mercury sources subject to methylation and bioaccumulation, recent studies have begun to utilize $\Delta^{200}\text{Hg}$ values in fish to verify the degree and the form of atmospheric mercury input (litterfall-versus precipitation-derived mercury) to aquatic environments (e.g., Lepak et al., 2018; Woerndle et al., 2018). Interestingly, the $\Delta^{200}\text{Hg}$ of the control food pellets and the fish tissues (0.23 – 0.74‰ ; Table S1) were the highest values ever recorded from fish (up to 0.19‰ ; reviewed in Kwon et al., 2020) and were comparable with precipitation (up to 1.30‰ ; reviewed in Cai and Chen, 2015). Given that precipitation is the major source of mercury to the open ocean (Blum et al., 2013; Mason and Fitzgerald, 1994), seawater samples collected from the Arctic coast and various U.S. sampling campaigns (exact locations unknown) have shown $\Delta^{200}\text{Hg}$ up to 0.53‰ (Strok et al., 2014, 2015). The process(es) resulting in such elevated $\Delta^{200}\text{Hg}$ in our control treatment is difficult to explain given the low average annual precipitation in the region where the anchovy and pompano were caught (west coast of Chile and Peru; Tapley and Waylen, 1990). At the moment, we speculate that anchovy, a filter feeder in the surface water column (Leong and O'Connell, 1969), may be more prone to direct uptake and bioaccumulation of precipitation-derived mercury from the seawater.

3.3. Isotopic compositions of the MeHg treatment

The food pellets spiked with varying MeHg concentrations displayed much lower $\delta^{202}\text{Hg}$ and $\Delta^{199}\text{Hg}$ relative to the mercury unamended food pellets (Fig. 1A). Synthetic mercury derived or used during industrial processes have been characterized by near-zero $\Delta^{199}\text{Hg}$ and negative $\delta^{202}\text{Hg}$ (Laffont et al., 2011; R. Sun et al., 2016). Previous fish feeding experiments have also observed near-zero $\Delta^{199}\text{Hg}$ and negative $\delta^{202}\text{Hg}$ in food pellets spiked with synthetic MeHg (Feng et al., 2015; Kwon et al., 2012). When compared to the MeHg_high food pellets, the MeHg_low food pellets showed intermediate $\Delta^{199}\text{Hg}$ between the control and MeHg_high food pellets (Fig. 1A). There was also $\sim 0.47\text{‰}$ shifts (greater than the analytical uncertainty; 2SD) in $\delta^{202}\text{Hg}$ from the binary mixing line between the control and MeHg_high food pellets (Fig. 1A), which is described by the equation

$${}^{\text{xxx}}\text{Hg}_{\text{MeHg_low}} = {}^{\text{xxx}}\text{Hg}_{\text{MeHg_high}} f_{\text{MeHg_high}} + {}^{\text{xxx}}\text{Hg}_{\text{control}} f_{\text{control}} \quad (5)$$

where ${}^{\text{xxx}}\text{Hg}$ represents either $\delta^{202}\text{Hg}$ or $\Delta^{199}\text{Hg}$, and f represents the fraction of THg concentration in either control or MeHg_high food pellets. The low % MeHg ($\sim 60\%$; Table 1) and the intermediate $\Delta^{199}\text{Hg}$ observed in the MeHg_low food pellets suggest that these

food pellets have not equilibrated completely to synthetic MeHg. The positive $\delta^{202}\text{Hg}$ shifts are consistent with microbial demethylation, resulting in a higher $\delta^{202}\text{Hg}$ in the remaining MeHg compared to the product IHg (Kritee et al., 2009). We speculate that there was microbial MeHg degradation in the MeHg_low food pellets possibly after the feeding experiment and during storage prior to the analyses of the food pellets. It is possible that microbial MeHg degradation has also occurred in the MeHg_high food pellets. Assuming that the degradation rate was the same between the two food pellets, the fraction of MeHg degraded in the MeHg_high food pellet would be smaller due to the larger MeHg mass in the MeHg_high food pellet compared to the MeHg_low food pellet. Thus, the small MDF resulted from microbial degradation may explain the absence of significant $\delta^{202}\text{Hg}$ shift in the MeHg_high food pellets.

After 10 weeks, all fish tissues from the MeHg_high treatment equilibrated to the isotopic compositions of their respective food pellets (Fig. 1A), suggesting that MeHg is efficiently assimilated and distributed to various tissues of fish (Leaner and Mason, 2004; Rabenstein and Evans, 1978). The fish tissues from the MeHg_low treatment also equilibrated to the isotopic compositions of the MeHg_high food pellets rather than the MeHg_low food pellets. Among the muscle tissues, we observed statistically no significant difference between the MeHg_low and MeHg_high treatments (Kruskal-Wallis test; $p = 0.83$ for both $\delta^{202}\text{Hg}$ and $\Delta^{199}\text{Hg}$), suggesting that they have both equilibrated to synthetic MeHg. A noticeable difference was observed in the mercury isotope ratios between the two replicate analyses of pooled kidney samples (Fig. 1A, Table S1). This is likely caused by the difficulty of sample homogenization for samples with high oil content. The $\delta^{202}\text{Hg}$ and $\Delta^{199}\text{Hg}$ of the replicate analyses were however on the binary mixing line, suggesting that the kidney tissues have bioaccumulated experimentally spiked synthetic MeHg.

The equilibration of the isotopic compositions of the MeHg_low fish tissues to the MeHg_high food pellets appears to reflect the preferential trophic transfer and bioaccumulation of synthetic MeHg with lower $\delta^{202}\text{Hg}$ and $\Delta^{199}\text{Hg}$ to the fish tissues and excretion of IHg from the food pellets with higher $\delta^{202}\text{Hg}$ and $\Delta^{199}\text{Hg}$. The major difference between the MeHg_high ($\sim 95\%$ MeHg) and MeHg_low food pellets ($\sim 60\%$ MeHg) was the % MeHg value. In a previous fish feeding experiment, the muscle tissues of yellow perch, when fed food pellets spiked with high MeHg concentrations, equilibrated to the isotopic compositions of their respective food pellets within two months, consistent with our MeHg_high treatments (Kwon et al., 2012). In the same study, the muscle tissues of yellow perch fed food pellets composed of $\sim 70\%$ MeHg and $\sim 30\%$ IHg showed measurable isotopic discrepancies between the fish and the food pellets, similar to our MeHg_low treatments. The authors suggested that this reflects the preferential trophic transfer of MeHg isotopic composition and the food pellets display mixtures of IHg and MeHg isotopic compositions. Given that the fish tissues from the MeHg_low treatment had similarly elevated % MeHg compared to the MeHg_high treatment, the trophic transfer of synthetic MeHg explains the isotopic deviation between the food and the fish. We also note that, while the potential MDF in fish cannot be disregarded, the overwhelming of the fish tissues with the isotopic composition of a high MeHg diet would obscure any signs of MDF in fish.

3.4. Isotopic compositions in the IHg treatment

The food pellets spiked with varying IHg concentrations displayed much lower $\delta^{202}\text{Hg}$ and $\Delta^{199}\text{Hg}$ compared to the control diet (Fig. 1B), consistent with synthetic mercury derived or used during industrial processes (Laffont et al., 2011; R. Sun et al., 2016). The

IHg_low and IHg_high food pellets showed similar mercury isotope ratios and low % MeHg (6–20%), suggesting that they have both equilibrated to synthetic IHg. After 10 week, there was a complete equilibration of mercury isotopic compositions of the intestine to the isotopic compositions of the IHg_low and IHg_high food pellets (Fig. 1B). The remaining tissues of the muscle, kidney, and liver exhibited varying shifts in $\delta^{202}\text{Hg}$ and $\Delta^{199}\text{Hg}$ toward the IHg food pellets (Fig. 1B), consistent with the varying changes in % MeHg (Table 1). By plotting % MeHg against $\delta^{202}\text{Hg}$ and $\Delta^{199}\text{Hg}$ of the fish tissues, we estimate that the variability in MeHg fractions is responsible for 70–92% of the tissue-specific variation in mercury isotope ratios (Fig. 2). In the liver tissues, we also observed additional $\sim 0.63\%$ shifts in $\delta^{202}\text{Hg}$ (greater than the analytical uncertainty; 2SD) from the binary mixing line between the control liver and the IHg_high food pellets (Fig. 1B), which is described by the equation

$${}^{\text{xxx}}\text{Hg}_{\text{Ihg liver}} = {}^{\text{xxx}}\text{Hg}_{\text{IHg_high food pellet}} f_{\text{IHg_high food pellet}} + {}^{\text{xxx}}\text{Hg}_{\text{control liver}} f_{\text{control liver}} \quad (6)$$

where ${}^{\text{xxx}}\text{Hg}$ represents either $\delta^{202}\text{Hg}$ or $\Delta^{199}\text{Hg}$, and f represents the fraction of THg concentration in either the IHg_high food pellets or control liver.

Our results are consistent with pharmacokinetics studies of fish, which demonstrated the preferential binding of IHg to the intestine and slower increases in IHg in the muscle and other visceral organs when exposed to an IHg diet (Boudou et al., 1985; Feng et al., 2015; Pentreath, 1976a, 1976b). Histopathological studies have shown widespread binding of IHg across the epithelial surface and intestinal villi and MeHg was bound to small and more specific regions of the epithelial surface (Oliveira Ribeiro et al., 2002). Muscle and kidney are known to be the final storage and excretion organs for mercury (Berndt et al., 1985; Leaner and Mason, 2004), respectively, which explain the small increases in THg concentrations, small reductions in % MeHg, and small isotopic shifts toward the IHg food pellets observed in the muscle and kidney tissues. The muscle tissues from the IHg_high treatment exhibited varying isotopic shifts towards the IHg food pellets, which is well explained by their % MeHg such that the individual muscle with a higher IHg proportion shifted further towards the IHg food pellets. Liver is thought to respond rapidly to IHg exposure (Evans et al., 1993) and as evidenced by the elevated liver to muscle THg ratios (>1). The large increases in THg concentrations, large reductions in % MeHg, and

moderate isotopic shifts toward the IHg food pellets further confirm that liver is an effective indicator for assessing the degree and changes in IHg exposure from the environment.

In regards to identifying IHg sources using the fish liver, the positive $\delta^{202}\text{Hg}$ shifts from the binary mixing line suggest that there is a presence of complex internal process leading to a significant MDF and this internal process may obscure the isotopic composition of IHg sources. Our observation is consistent with the past experimental studies, which exposed fish with either IHg-spiked food pellets or natural diets containing IHg (Feng et al., 2015; Kwon et al., 2013). In particular, Feng et al. (2015) observed positive and negative $\delta^{202}\text{Hg}$ shifts in the liver and brain of fish, respectively, and suggested that the preferential redistribution of IHg with a lighter $\delta^{202}\text{Hg}$ from the liver to brain is responsible for the observed $\delta^{202}\text{Hg}$ shifts. In contrast, a recent field study documented significantly higher $\delta^{202}\text{Hg}$ (but not $\Delta^{199}\text{Hg}$) in the muscle compared to the liver of fish collected from sites contaminated by metallic mercury (mostly IHg) in Norwegian fjords (Rua-Ibarz et al., 2019). The authors attributed this to internal demethylation in the liver followed by the distribution MeHg with a higher $\delta^{202}\text{Hg}$ to the muscle.

We propose that the positive $\delta^{202}\text{Hg}$ shift in the fish liver is caused by the preferential redistribution of IHg with a lower $\delta^{202}\text{Hg}$ rather than internal demethylation. Our fish fed IHg food pellets were exposed to only small amounts of MeHg over the course of the experiment. We presume that internal demethylation of this small amounts of MeHg is unlikely to impart such measurable MDF. Even if there was internal demethylation, the isotopic composition of the IHg food pellets would overwhelm the potential MDF given the rapid response of liver to IHg exposure. Previous studies have also documented internal demethylation in the intestines of fish (Wang et al., 2017a; Wang and Wang, 2017) but not in the liver (Wang et al., 2013).

The evidence of IHg redistribution from the liver has been documented by many previous studies. *In vivo* and *in vitro* experiments reported significant reductions in liver IHg concentrations coupled with large increases in bile IHg concentrations (Ballatori and Clarkson, 1984, 1985; Ballatori, 1991). These studies also found that glutathione, due to its high abundance in the liver and strong binding affinity toward IHg, is the major mediator for IHg secretion into bile. IHg bound to thiol-ligands have been characterized by a lower $\delta^{202}\text{Hg}$ compared to unbound IHg in solution (Wiederhold et al., 2010). It is possible that the binding of a lighter $\delta^{202}\text{Hg}$ with glutathione followed by secretion into bile may result

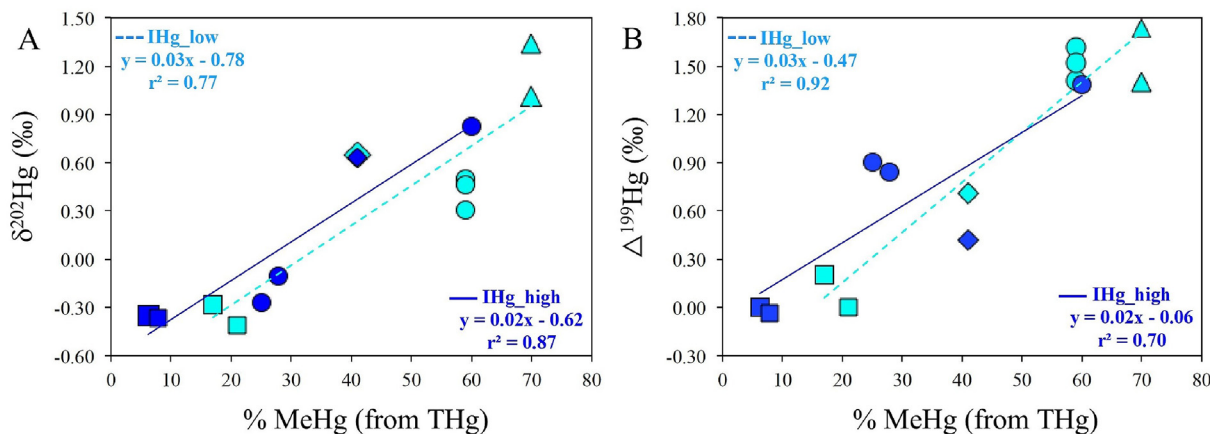


Fig. 2. A) $\delta^{202}\text{Hg}$ and B) $\Delta^{199}\text{Hg}$ against % MeHg of the tissues in the IHg_low (bright blue) and IHg_high (dark blue) treatments. Each symbol represents tissues of liver (diamond), intestine (square), kidney (triangle), and muscle (circle). Individual data point of liver and kidney represents a sample pooled from three individual fish. Individual data point of muscle and intestine represents a sample from one individual fish. The kidney from the IHg_high treatment is missing due to the small sample mass.

in a higher $\delta^{202}\text{Hg}$ in the liver. While the IHg-glutathione complex is known to drain back into the intestine via bile, this is unlikely to shift the $\delta^{202}\text{Hg}$ of intestine given that the intestine is overwhelmed by the isotopic composition of the dietary IHg. The absence of negative $\delta^{202}\text{Hg}$ shifts in the muscle and kidney also corresponds with the preferential excretion of IHg and small observed changes in THg concentrations and % MeHg in these tissues. Additionally, Li et al. (2020) documented a positive $\delta^{202}\text{Hg}$ shift in the liver of adult pilot whale only when the liver accumulated high levels of IHg. The authors concluded that the preferential redistribution of a labile IHg to other tissues explains the observed positive $\delta^{202}\text{Hg}$ shift. We therefore postulate that the mechanism of hepatic IHg metabolism is perhaps similar between marine fish and mammals when exposed to high dietary IHg sources.

4. Conclusions

In summary, we observed absence of significant MDF and MIF_{odd} in the tissues of fish when fed food pellets composed mainly of MeHg (control and MeHg treatments). This suggests that the potential MDF occurring in fish may be diluted by the isotopic composition of the dietary MeHg, which is efficiently assimilated and integrated into various fish tissues. Even under environmentally relevant THg and MeHg exposure (control fish), the tissue-specific variation in mercury isotope ratios resulted primarily by the varying MeHg fraction suggests that we can confidently use mercury isotope ratios in fish tissues to trace sources and biogeochemical processes of mercury in natural ecosystems.

This study provides insights into how a variety of fish tissues respond under different mercury species and under three different mercury pollution scenarios (IHg vs MeHg vs natural). Aquatic ecosystems that are characterized as contaminated typically have elevated IHg concentrations and limited MeHg production capabilities in aquatic matrices (Colombo et al., 2013; Zhao et al., 2016). At these sites, mercury concentration in fish liver has been used as a bioindicator for the extent of IHg pollution. We found that, while the liver tissues of fish fed IHg amended food pellets show moderate increases in THg concentrations, the positive $\delta^{202}\text{Hg}$ shifts indicate that fish liver is not a conservative tracer for IHg sources. The incomplete isotopic equilibration in the muscle and kidney also makes them difficult to be used for IHg source tracing. Instead, the intestines of fish accumulate substantial amounts of dietary IHg and undergo complete equilibration to the isotopic composition of the dietary IHg. We therefore suggest that among all tissues examined in this study, fish intestine is the most suitable proxy for identifying sources of IHg at polluted sites. These results are essential for determining the appropriate tissues of Olive flounder and other species of marine fish for monitoring environmental sources of IHg and MeHg. Based on this study and latest research on mercury metabolism in fish and marine mammals (e.g., Li et al., 2020; Feng et al., 2015), we encourage more research to evaluate the influence of environmental factors (i.e., selenium levels) affecting internal demethylation and to enhance the interpretation of the tissue-specific variation in mercury isotope ratios in nature. Expanding the tissue type and sample size, which allows detailed statistical analyses, would also improve the understanding of subtle differences in tissue-specific variation in mercury isotope ratios.

Author Statement

Bong Joo Lee: Fish feeding experiment, Writing. Sae Yun Kwon: Conceptualization, Writing. Runsheng Yin: Isotope analysis, Writing. Miling Li: Data interpretation, Writing. Saebom Jung: Sample preparation, Data acquisition, Data visualization. Seung Hyeon Lim: Sample preparation, Data acquisition, Data

visualization. Ju Hyeon Lee: Sample preparation, Data acquisition, Data visualization. Kang Woong Kim: Study concept, Fish feeding experiment. Kyoung Duck Kim: Study concept, Fish feeding experiment. Ji Wong Jang: Fish feeding experiment, Dissection.

Declaration of competing interest

The authors declare that they have no known competing financial interests or personal relationships that could have appeared to influence the work reported in this paper.

Acknowledgments

No conflict of interest to declare. This work was supported by the National Institute of Fisheries Science, South Korea [grant number R2019013]; the National Research Foundation of Korea (NRF) funded by the Korea government (MSIT) [grant number NRF-2019R1F1A1058928]; the Korea Institute of Ocean Science and Technology [grant number PE99883]; the National Institute of Environmental Research (NIER) funded by the Korea government [grant number NIER-2020-01-01-086]; and the POSTECH Basic Science Research Institute Grant.

Appendix A. Supplementary data

Supplementary data to this article can be found online at <https://doi.org/10.1016/j.envpol.2020.115588>.

References

- Ballatori, N., Clarkson, T.W., 1984. Inorganic mercury secretion into bile as a low molecular weight complex. *Biochem. Pharmacol.* 33, 1087–1092.
- Ballatori, N., Clarkson, T.W., 1985. Biliary secretion of glutathione and of glutathione-metal complexes. *Toxicol. Sci.* 5, 816–831.
- Ballatori, N., 1991. Mechanisms of metal transport across liver cell plasma membranes. *Drug Metab. Rev.* 23, 83–132.
- Bergquist, B.A., Blum, J.D., 2007. Mass-dependent and-independent fractionation of Hg isotopes by photoreduction in aquatic systems. *Science* 318, 417–420.
- Berndt, W.O., Baggett, J.M., Blacker, A., Houser, M., 1985. Renal glutathione and mercury uptake by kidney. *Toxicol. Sci.* 5, 832–839.
- Blum, J.D., Bergquist, B.A., 2007. Reporting of variations in the natural isotopic composition of mercury. *Anal. Bioanal. Chem.* 388, 353–359.
- Blum, J.D., Popp, B.N., Drazen, J.C., Choy, C.A., Johnson, M.W., 2013. Methylmercury production below the mixed layer in the North Pacific ocean. *Nat. Geosci.* 6, 879–884.
- Blum, J.D., Sherman, L.S., Johnson, M.W., 2014. Mercury isotopes in earth and environmental sciences. *Annu. Rev. Earth Planet Sci.* 42, 249–269.
- Blum, J.D., Johnson, M.W., 2017. Recent developments in mercury stable isotope analysis. *Rev. Mineral. Geochem.* 82, 733–757.
- Bolea-Fernandez, E., Rua-Ibarz, A., Krupp, E.M., Feldmann, J., Vanhaecke, F., 2019. High-precision isotopic analysis sheds new light on mercury metabolism in long-finned pilot whales (*Globicephala melas*). *Sci. Rep.* 9, 1–10.
- Boudou, A., Ribeyre, F., 1985. Experimental study of trophic contamination of *Salmo gairdneri* by two mercury compounds— HgCl_2 and CH_3HgCl —analysis at the organism and organ levels. *Water Air Soil Pollut.* 26, 137–148.
- Cai, H., Chen, J., 2016. Mass-independent fractionation of even mercury isotopes. *Sci. Bull.* 61, 116–124.
- Chen, J., Hintelmann, H., Feng, X., Dimock, B., 2012. Unusual fractionation of both odd and even mercury isotopes in precipitation from Peterborough, ON, Canada. *Geochem. Cosmochim. Acta* 90, 33–46.
- Choi, J.H., Yoon, S.C., Lee, S.I., Kim, J.B., Kim, H.R., 2011. Feeding habits of *Paralichthys olivaceus* in the Uljin marine ranching area. *Korean J. Fish. Aquat. Sci.* 44, 684–688.
- Cizdziel, J., Hinners, T., Cross, C., Pollard, J., 2003. Distribution of mercury in the tissues of five species of freshwater fish from Lake Mead, USA. *J. Environ. Monit.* 5, 802–807.
- Colombo, M.J., Ha, J., Reinfelder, J.R., Barkay, T., Yee, N., 2013. Anaerobic oxidation of Hg (0) and methylmercury formation by *Desulfovibrio desulfuricans* ND132. *Geochem. Cosmochim. Acta* 112, 166–177.
- Cransveld, A., Amouroux, D., Tessier, E., Koutrakis, E., Ozturk, A.A., Bettoso, N., Mieiro, C.L., Berail, S., Barre, J.P., Sturaro, N., Schnitzler, J., 2017. Mercury stable isotopes discriminate different populations of European seabass and trace potential Hg sources around Europe. *Environ. Sci. Technol.* 51, 12219–12228.
- Donovan, P.M., Blum, J.D., Singer, M.B., Marvin-DiPasquale, M., Tsui, M.T., 2016. Isotopic composition of inorganic mercury and methylmercury downstream of

- a historical gold mining region. *Environ. Sci. Technol.* 50, 1691–1702.
- Eagles-Smith, C.A., Ackerman, J.T., Willacker, J.J., Tate, M.T., Lutz, M.A., Fleck, J.A., Stewart, A.R., Wiener, J.G., Evers, D.C., Lepak, J.M., Davis, J.A., 2016. Spatial and temporal patterns of mercury concentrations in freshwater fish across the Western United States and Canada. *Sci. Total Environ.* 568, 1171–1184.
- Eckley, C.S., Hintelmann, H., 2006. Determination of mercury methylation potentials in the water column of lakes across Canada. *Sci. Total Environ.* 368, 111–125.
- Entwisle, J., Malinovsky, D., Dunn, P.J., Goenaga-Infante, H., 2018. Hg isotope ratio measurements of methylmercury in fish tissues using HPLC with off line cold vapour generation MC-ICPMS. *J. Anal. Atomic Spectrom.* 33, 1645–1654.
- Epov, V.N., Rodriguez-Gonzalez, P., Sonke, J.E., Tessier, E., Amouroux, D., Bourgoin, L.M., Donard, O.F., 2008. Simultaneous determination of species-specific isotopic composition of Hg by gas chromatography coupled to multi-collector ICPMS. *Anal. Chem.* 80, 3530–3538.
- Evans, D.W., Dodo, D.K., Hanson, P.J., 1993. Trace element concentrations in fish livers: implications of variations with fish size in pollution monitoring. *Mar. Pollut. Bull.* 26, 329–334.
- Feng, C., Pedrero, Z., Gentès, S., Barre, J., Renedo, M., Tessier, E., Bérail, S., Maury-Brachet, R., Mesmer-Dudons, N., Baudrimont, M., Legeay, A., 2015. Specific pathways of dietary methylmercury and inorganic mercury determined by mercury speciation and isotopic composition in zebrafish (*Danio rerio*). *Environ. Sci. Technol.* 49, 12984–12993.
- Gehrke, G.E., Blum, J.D., Marvin-DiPasquale, M., 2011. Sources of mercury to San Francisco Bay surface sediment as revealed by mercury stable isotopes. *Geochim. Cosmochim. Acta* 75, 691–705.
- Gilmour, C.C., Henry, E.A., Mitchell, R., 1992. Sulfate stimulation of mercury methylation in freshwater sediments. *Environ. Sci. Technol.* 26, 2281–2287.
- Hammerschmidt, C.R., Fitzgerald, W.F., 2006. Methylmercury in freshwater fish linked to atmospheric mercury deposition. *Environ. Sci. Technol.* 40, 7764–7770.
- Janssen, S.E., Johnson, M.W., Blum, J.D., Barkay, T., Reinfelder, J.R., 2015. Separation of monomethylmercury from estuarine sediments for mercury isotope analysis. *Chem. Geol.* 411, 19–25.
- Kritee, K., Barkay, T., Blum, J.D., 2009. Mass dependent stable isotope fractionation of mercury during mer mediated microbial degradation of monomethylmercury. *Geochim. Cosmochim. Acta* 73, 1285–1296.
- Kwon, S.Y., Blum, J.D., Carvan, M.J., Basu, N., Head, J.A., Madenjian, C.P., David, S.R., 2012. Absence of fractionation of mercury isotopes during trophic transfer of methylmercury to freshwater fish in captivity. *Environ. Sci. Technol.* 46, 7527–7534.
- Kwon, S.Y., Blum, J.D., Chirby, M.A., Chesney, E.J., 2013. Application of mercury isotopes for tracing trophic transfer and internal distribution of mercury in marine fish feeding experiments. *Environ. Toxicol. Chem.* 32, 2322–2330.
- Kwon, S.Y., Blum, J.D., Chen, C.Y., Meattay, D.E., Mason, R.P., 2014. Mercury isotope study of sources and exposure pathways of methylmercury in estuarine food webs in the Northeastern US. *Environ. Sci. Technol.* 48, 10089–10097.
- Kwon, S.Y., Blum, J.D., Nadelhoffer, K.J., Dvonch, J.T., Tsui, M.T.K., 2015. Isotopic study of mercury sources and transfer between a freshwater lake and adjacent forest food web. *Sci. Total Environ.* 532, 220–229.
- Kwon, S.Y., Blum, J.D., Madigan, D.J., Block, B.A., Popp, B.N., 2016. Quantifying mercury isotope dynamics in captive Pacific bluefin tuna (*Thunnus orientalis*). *Elementa-Sci Anthropol* 4, 1–15.
- Kwon, S.Y., Blum, J.D., Yin, R., Tsui, M.T.K., Yang, Y.H., Choi, J.W., 2020. Mercury stable isotopes for monitoring the effectiveness of the Minamata Convention on Mercury. *Earth Sci. Rev.* 203, 1–22.
- Laffont, L., Sonke, J.E., Maurice, L., Monroy, S.L., Chincheros, J., Amouroux, D., Behra, P., 2011. Hg speciation and stable isotope signatures in human hair as a tracer for dietary and occupational exposure to mercury. *Environ. Sci. Technol.* 45, 9910–9916.
- Leaner, J.J., Mason, R.P., 2004. Methylmercury uptake and distribution kinetics in sheepshead minnows, *Cyprinodon variegatus*, after exposure to CH₃Hg-spiked food. *Environ. Toxicol. Chem.* 23, 2138–2146.
- Leong, R.J., O'Connell, C.P., 1969. A laboratory study of particulate and filter feeding of the northern anchovy (*Engraulis mordax*). *Can. J. Fish. Aquat. Sci.* 26, 557–582.
- Lepak, R.F., Janssen, S.E., Yin, R., Krabbenhoft, D.P., Ogorek, J.M., DeWild, J.F., Tate, M.T., Holsen, T.M., Hurley, J.P., 2018. Factors affecting mercury stable isotopic distribution in piscivorous fish of the Laurentian Great Lakes. *Environ. Sci. Technol.* 52, 2768–2776.
- Li, M., Sherman, L.S., Blum, J.D., Grandjean, P., Mikkelsen, B., Weihe, P., Sunderland, E.M., Shine, J.P., 2014. Assessing sources of human methylmercury exposure using stable mercury isotopes. *Environ. Sci. Technol.* 48, 8800–8806.
- Li, M., Juang, C.A., Ewald, J.D., Yin, R., Mikkelsen, B., Krabbenhoft, D.P., Balcom, P.H., Dassuncao, C., Sunderland, E.M., 2020. Selenium and stable mercury isotopes provide new insights into mercury toxicokinetics in pilot whales. *Sci. Total Environ.* 710, 136325.
- Masbou, J., Sonke, J.E., Amouroux, D., Guillou, G., Becker, P.R., Point, D., 2018. Hg-Stable isotope variations in marine top predators of the western Arctic ocean. *ACS Earth Space Chem.* 2, 479–490.
- Mason, R.P., Fitzgerald, W.F., Morel, F.M., 1994. The biogeochemical cycling of elemental mercury: anthropogenic influences. *Geochim. Cosmochim. Acta* 58, 3191–3198.
- McCloskey, J.T., Schultz, I.R., Newman, M.C., 1998. Estimating the oral bioavailability of methylmercury to channel catfish (*Ictalurus punctatus*). *Environ. Toxicol. Chem.* 17, 1524–1529.
- Oliveira Ribeiro, C.A., Rouleau, C., Pelletier, E., Audet, C., Tjälve, H., 1999. Distribution kinetics of dietary methylmercury in the arctic charr (*Salvelinus alpinus*). *Environ. Sci. Technol.* 33, 902–907.
- Oliveira Ribeiro, C.A., Belger, L., Pelletier, E., Rouleau, C., 2002. Histopathological evidence of inorganic mercury and methyl mercury toxicity in the arctic charr (*Salvelinus alpinus*). *Environ. Res.* 90, 217–225.
- Pentreath, R.J., 1976a. The accumulation of mercury from food by the plaice, *Pleuronectes platessa* L. *J. Exp. Mar. Biol. Ecol.* 25, 51–65.
- Pentreath, R.J., 1976b. The accumulation of inorganic mercury from sea water by the plaice, *Pleuronectes platessa* L. *J. Exp. Mar. Biol. Ecol.* 24, 103–119.
- Perrot, V., Masbou, J., Pastukhov, M.V., Epov, V.N., Point, D., Bérail, S., Becker, P.R., Sonke, J.E., Amouroux, D., 2016. Natural Hg isotopic composition of different Hg compounds in mammal tissues as a proxy for in vivo breakdown of toxic methylmercury. *Metal* 8, 170–178.
- Perrot, V., Landing, W.M., Grubbs, R.D., Salters, V.J., 2019. Mercury bioaccumulation in tilefish from the northeastern Gulf of Mexico 2 years after the Deepwater Horizon oil spill: insights from Hg, C, N and S stable isotopes. *Sci. Total Environ.* 666, 828–838.
- Rabenstein, D.L., Evans, C.A., 1978. The mobility of methylmercury in biological systems. *Bioinorg. Chem. Appl.* 8, 107–114.
- Rodríguez-González, P., Epov, V.N., Bridor, R., Tessier, E., Guyoneaud, R., Monperrus, M., Amouroux, D., 2009. Species-specific stable isotope fractionation of mercury during Hg (II) methylation by an anaerobic bacteria (*Desulfobolbus propionicus*) under dark conditions. *Environ. Sci. Technol.* 43, 9183–9188.
- Rua-Ibarz, A., Bolea-Fernandez, E., Maage, A., Frantzen, S., Sanden, M., Vanhaecke, F., 2019. Tracing mercury pollution along the Norwegian coast via elemental, speciation, and isotopic analysis of liver and muscle tissue of deep-water marine fish (*Brosme brosme*). *Environ. Sci. Technol.* 53, 1776–1785.
- Rudd, J.W., Furutani, A.K.I.R.A., Turner, M.A., 1980. Mercury methylation by fish intestinal contents. *Appl. Environ. Microbiol.* 40, 777–782.
- Sherman, L.S., Blum, J.D., 2013. Mercury stable isotopes in sediments and large-mouth bass from Florida lakes, USA. *Sci. Total Environ.* 448, 163–175.
- Streets, D.G., Horowitz, H.M., Lu, Z., Levin, L., Thackray, C.P., Sunderland, E.M., 2019. Five hundred years of anthropogenic mercury: spatial and temporal release profiles. *Environ. Res. Lett.* 14, 84004.
- Strok, M., Hintelmann, H., Dimock, B., 2014. Development of pre-concentration procedure for the determination of Hg isotope ratios in seawater samples. *Anal. Chim. Acta* 851, 57–63.
- Strok, M., Baya, P.A., Hintelmann, H., 2015. The mercury isotope composition of Arctic coastal seawater. *C R Geosci.* 347, 368–376.
- Sun, G., Sommar, J., Feng, X., Lin, C.J., Ge, M., Wang, W., Yin, R., Fu, X., Shang, L., 2016a. Mass-dependent and-independent fractionation of mercury isotope during gas-phase oxidation of elemental mercury vapor by atomic Cl and Br. *Environ. Sci. Technol.* 50, 9232–9241.
- Sun, R., Streets, D.G., Horowitz, H.M., Amos, H.M., Liu, G., Perrot, V., Toutain, J.P., Hintelmann, H., Sunderland, E.M., Sonke, J.E., 2016b. Historical (1850–2010) mercury stable isotope inventory from anthropogenic sources to the atmosphere. *Elementa-Sci Anthropol* 4, 1–15.
- Tapley Jr., T.D., Waylen, P.R., 1990. Spatial variability of annual precipitation and ENSO events in western Peru. *Hydro. Sci. J.* 35, 429–446.
- Wang, R., Feng, X.B., Wang, W.X., 2013. In vivo mercury methylation and demethylation in freshwater tilapia quantified by mercury stable isotopes. *Environ. Sci. Technol.* 47, 7949–7957.
- Wang, X., Wu, F., Wang, W.X., 2017. In vivo mercury demethylation in a marine fish (*Acanthopagrus schlegelii*). *Environ. Sci. Technol.* 51, 6441–6451.
- Wang, X., Wang, W.X., 2017. Selenium induces the demethylation of mercury in marine fish. *Environ. Pollut.* 231, 1543–1551.
- Wiederhold, J.G., Cramer, C.J., Daniel, K., Infante, I., Bourdon, B., Kretzschmar, R., 2010. Equilibrium mercury isotope fractionation between dissolved Hg (II) species and thiol-bound Hg. *Environ. Sci. Technol.* 44, 4191–4197.
- Woerndle, G.E., Tsz-Ki Tsui, M., Sebestyen, S.D., Blum, J.D., Nie, X., Kolka, R.K., 2018. New insights on ecosystem mercury cycling revealed by stable isotopes of mercury in water flowing from a headwater peatland catchment. *Environ. Sci. Technol.* 52, 1854–1861.
- Xu, X., Wang, W.X., 2015. Isotopic fractionation during the uptake and elimination of inorganic mercury by a marine fish. *Environ. Pollut.* 206, 202–208.
- Yin, R., Krabbenhoft, D.P., Bergquist, B.A., Zheng, W., Lepak, R.F., Hurley, J.P., 2016. Effects of mercury and thallium concentrations on high precision determination of mercury isotopic composition by Neptune Plus multiple collector inductively coupled plasma mass spectrometry. *J. Anal. Atomic Spectrom.* 31, 2060–2068.
- Zhao, L., Qiu, G., Anderson, C.W., Meng, B., Wang, D., Shang, L., Yan, H., Feng, X., 2016. Mercury methylation in rice paddies and its possible controlling factors in the Hg mining area, Guizhou province, Southwest China. *Environ. Pollut.* 215, 1–9.
- Zheng, W., Hintelmann, H., 2009. Mercury isotope fractionation during photoreduction in natural water is controlled by its Hg/DOC ratio. *Geochim. Cosmochim. Acta* 73, 6704–6715.